

Electronic supplementary information (ESI)

Switching on thermal and light-induced spin crossover by desolvation of the $[\text{Fe}(\text{3-bpp})_2](\text{XO}_4)_2 \cdot \text{solvent}$ ($\text{X} = \text{Cl, Re}$) compounds

Abdelhak Djemel,^{a,b} Olaf Stefanczyk,^{*a,c} Cédric Desplanches,^a Kunal Kumar,^c Rachid Delimi,^d Farouk Benaceur,^b Shin-ichi Ohkoshi,^c and Guillaume Chastanet^{*a}

^a CNRS, Univ. Bordeaux, Bordeaux INP, ICMCB, UMR 5026, 87 avenue du Dr. A. Schweitzer, Pessac, F-33608 (France).

^b Research Unit of Medicinal Plants (RUMP), University Pole No 02, Laghouat 3000, attached to Biotechnology Research Center (CRBt), UV 03 BP E73 Ali Mendjeli New Town, Constantine 25000 (Algeria).

^c Department of Chemistry, School of Science The University of Tokyo, 7-3-1 Hongo, Bunkyo-ku, Tokyo 113-0033 (Japan).

^d Badji Mokhtar University, Laboratory of Water Treatment and Valorization of Industrial Waste, BP 12, Annaba 23000 (Algeria).

E-mail OS: olaf@chem.s.u-tokyo.ac.jp. E-mail GS: guillaume.chastanet@icmcb.cnrs.fr.

Contents

Thermogravimetry.....	2
Figure S1. Thermogravimetric analyses of 1·sol (a) and 2·sol (b). Insets contain the first derivatives of the TGA curves (DTG)	2
Pictures of samples – desolvation induced colors changes.....	3
Figure S2. Pictures of 1·sol and 2·sol under different conditions: (a) freshly collected crystals, (b) crystallites after 5 min at 25°C, (c) samples just after heating to 120°C, (d) crystallites after 30 min at 120°C, (e) powdered samples for a total of 35 min at 120°C, and (f) powdered samples for a total of 90 min at 120°C.	3
Figure S3. Room temperature pictures of 1·sol and 2·sol spread on cellulose paper for the fresh sample, after 24 hours in air at ambient conditions and after 2 hours of heating at 120°C.	3
Infrared (IR) spectroscopy.....	4
Figure S4. Infrared (IR) absorption spectra in KBr of 3-bpp, NaClO ₄ ·H ₂ O, KReO ₄ , 1·sol and 2·sol (pristine, after 24 h in air at ambient conditions, and 2 h heated at 120°C) in: (a) the 4000 – 400 cm ⁻¹ range, and (b) the fingerprint region with assignment.....	4
Ultraviolet-visible-near infrared (UV-vis-NIR) spectroscopy.....	5
Figure S5. Room temperature solid-state UV–Vis–NIR absorption (Kubelka–Munk function) spectra with assignment of 3-bpp, NaClO ₄ ·H ₂ O, KReO ₄ , 1·sol (a) and 2·sol (b) (pristine, after 24 h in dry air, and 2 h heated at 120°C) dispersed in BaSO ₄	5
Computational details.....	6
Figure S6. Models of A (a), B (b) and C (c) used for quantum chemical calculations.....	6
Figure S7. Calculated UV-vis spectra of 1·sol (green), 2·sol (blue), and [Fe(3-bpp) ₂][Au(CN) ₂] ₂ ·2H ₂ O (red) base on models A , B and C , respectively. Bars indicate relative probability of electronic transitions.	7
Figure S8. The energy level diagram with Fe <i>d</i> -based representative low spin molecular orbitals calculated for 1·sol and 2·sol	8
List of excited state calculated for LS Fe(II)-based model A taken from complex 1·sol	8
List of excited state calculated for LS Fe(II)-based model B taken from complex 2·sol	10
Figure S9. The energy level diagram with Fe <i>d</i> -based representative high spin molecular orbitals calculated for input file taken from reference R2.	13
List of excited state calculated for HS Fe(II)-based model C taken from reference R2.	14
Single crystal X-ray diffraction (SCXRD) studies.....	17
Table S1. Selected crystallographic parameters for 1·sol and 2·sol	17
Table S2. Selected bond lengths and angles for 1·sol and 2·sol	17
Figure S10. Packing along crystallographic directions (100) (a for 1·sol and b for 2·sol), (010) (c for 1·sol and d for 2·sol), and (001) (e for 1·sol and f for 2·sol) including a hydrogen bond networks.	18
Powder X-ray diffraction (PXRD) studies.....	19
Figure S11. (a) Experimental PXRD patterns of 1·sol (pristine, after 24 h in dry air, and 2 h heated at 120°C) and calculated from single-crystal X-ray diffraction data including texture effect with preferred platy orientation along (002) direction with March-Dollase parameter <i>M/D</i> = 0.6 (1·sol*). (b) Time-evolution of diffractograms of pristine 1·sol . (c) Time-evolution of PXRD patterns of desolvated 1 (2 h heated at 120°C). (d) Experimental PXRD patterns of 2·sol (pristine and 2 h heated at 120°C) and calculated from single-crystal X-ray diffraction data (2·sol*). (e) Time-evolution of diffractograms of pristine 2·sol . (f) Time-evolution of PXRD patterns of desolvated 2 (2 h heated at 120°C).	19
Photomagnetic properties.....	20
Figure S12. Time dependence of $\chi_{\text{M}}T$ at $H_{\text{dc}} = 10$ kOe during excitation at 10 K with 650 nm light ($P = 5$ mW/cm ²) for pristine (1·sol) and desolvated phases (1 and 2).	20

Thermogravimetry

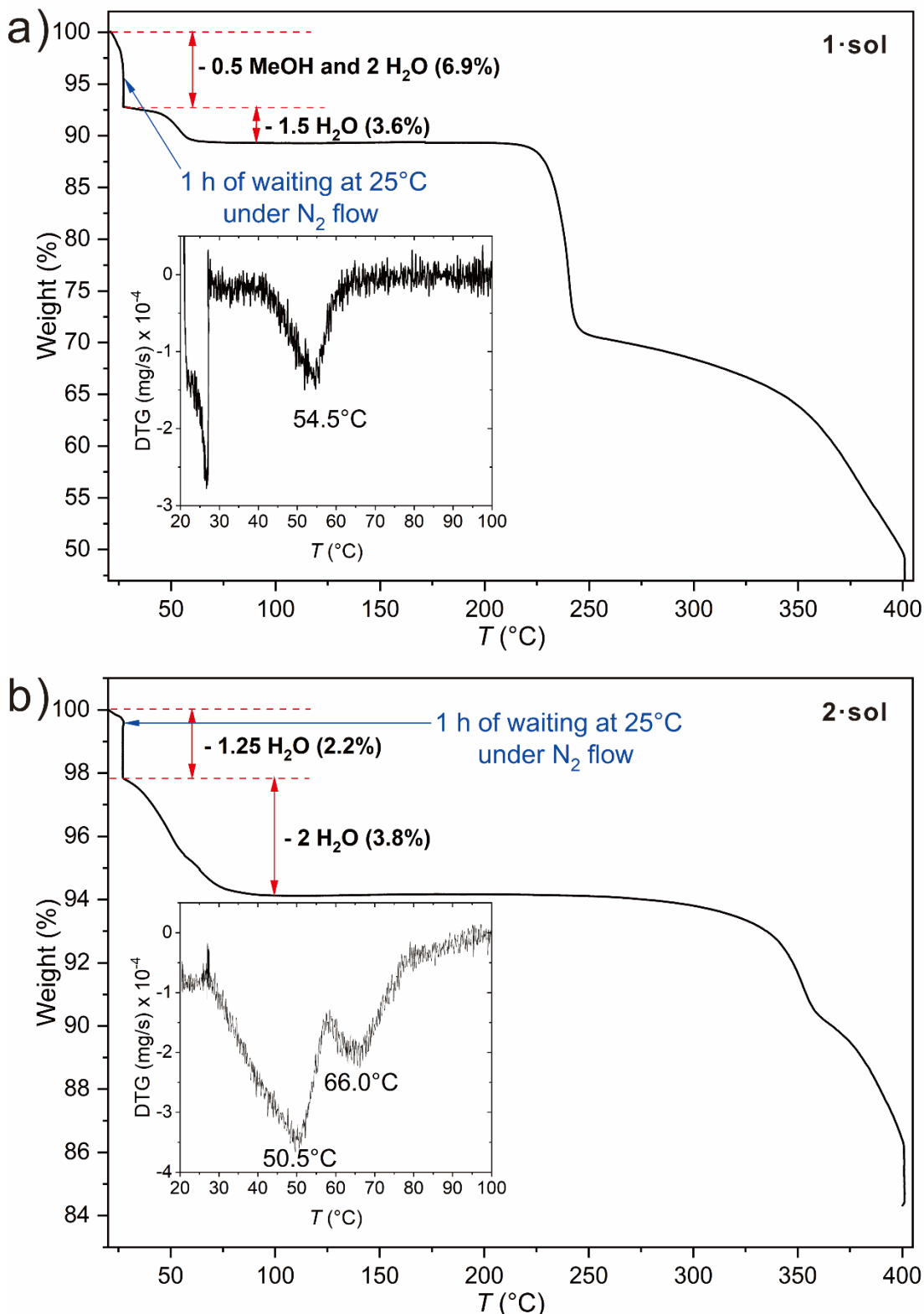


Figure S1. Thermogravimetric analyses of **1-sol** (a) and **2-sol** (b). Insets contain the first derivatives of the TGA curves (DTG).

Pictures of samples – desolvation induced colors changes

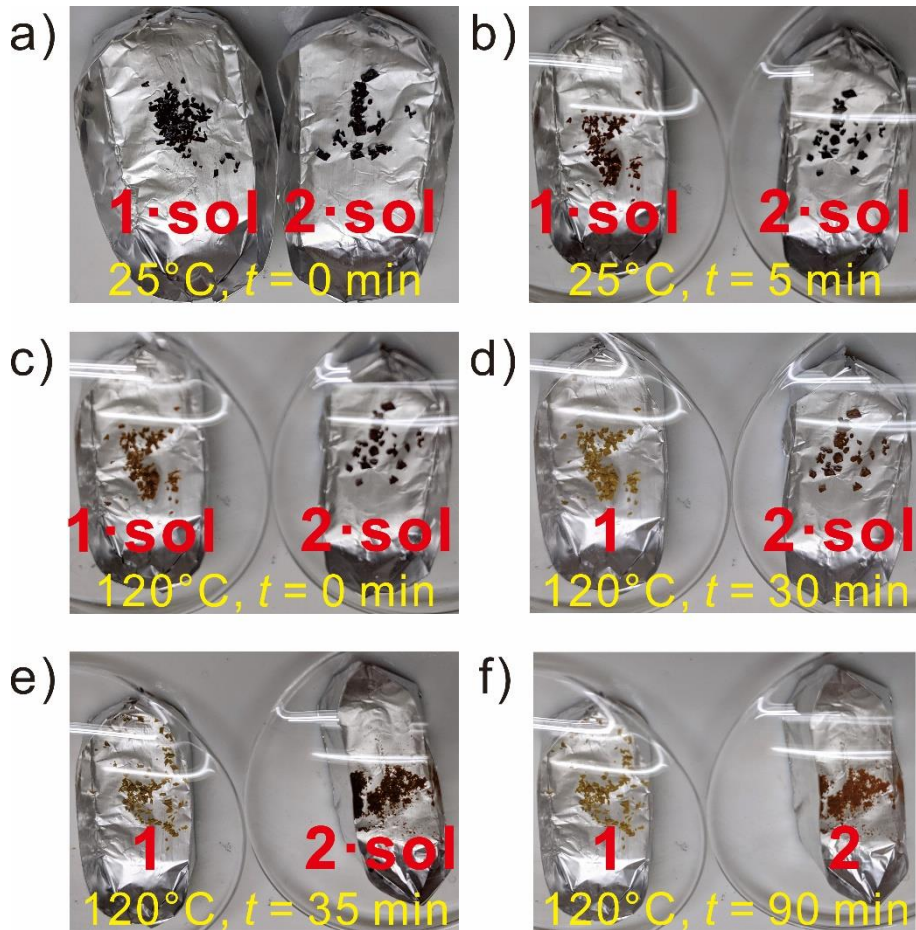


Figure S2. Pictures of **1-sol** and **2-sol** under different conditions: (a) freshly collected crystals, (b) crystallites after 5 min at 25°C, (c) samples just after heating to 120°C, (d) crystallites after 30 min at 120°C, (e) powdered samples for a total of 35 min at 120°C, and (f) powdered samples for a total of 90 min at 120°C.

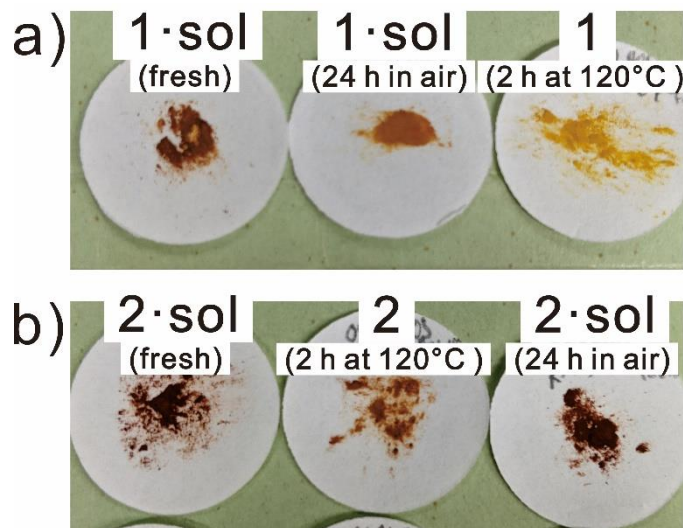


Figure S3. Room temperature pictures of **1-sol** and **2-sol** spread on cellulose paper for the fresh sample, after 24 hours in air at ambient conditions and after 2 hours of heating at 120°C.

Infrared (IR) spectroscopy

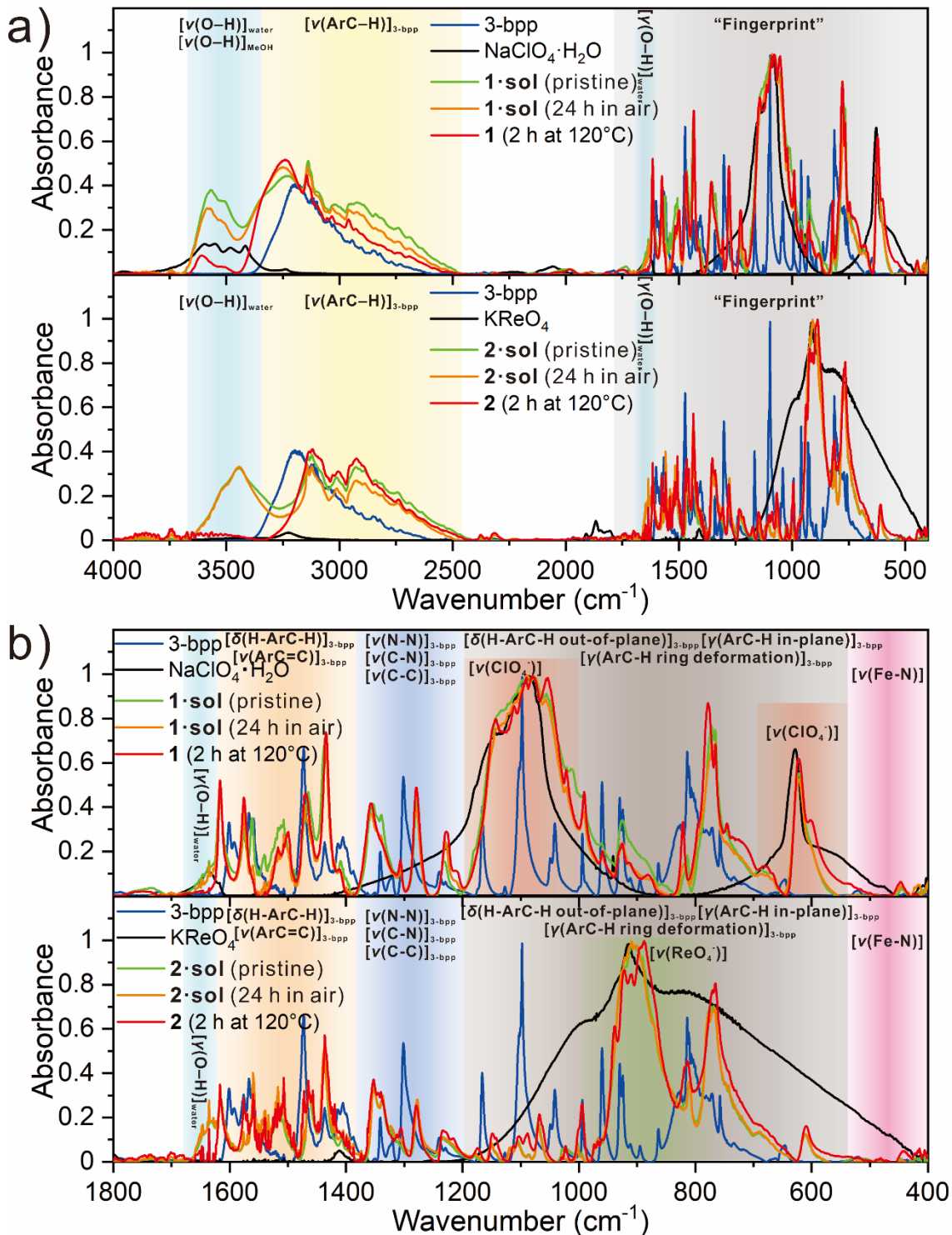


Figure S4. Infrared (IR) absorption spectra in KBr of 3-bpp, $\text{NaClO}_4 \cdot \text{H}_2\text{O}$, KReO_4 , **1·sol** and **2·sol** (pristine, after 24 h in air at ambient conditions, and 2 h heated at 120°C) in: (a) the 4000 – 400 cm^{-1} range, and (b) the fingerprint region with assignment.

Ultraviolet-visible-near infrared (UV-vis-NIR) spectroscopy

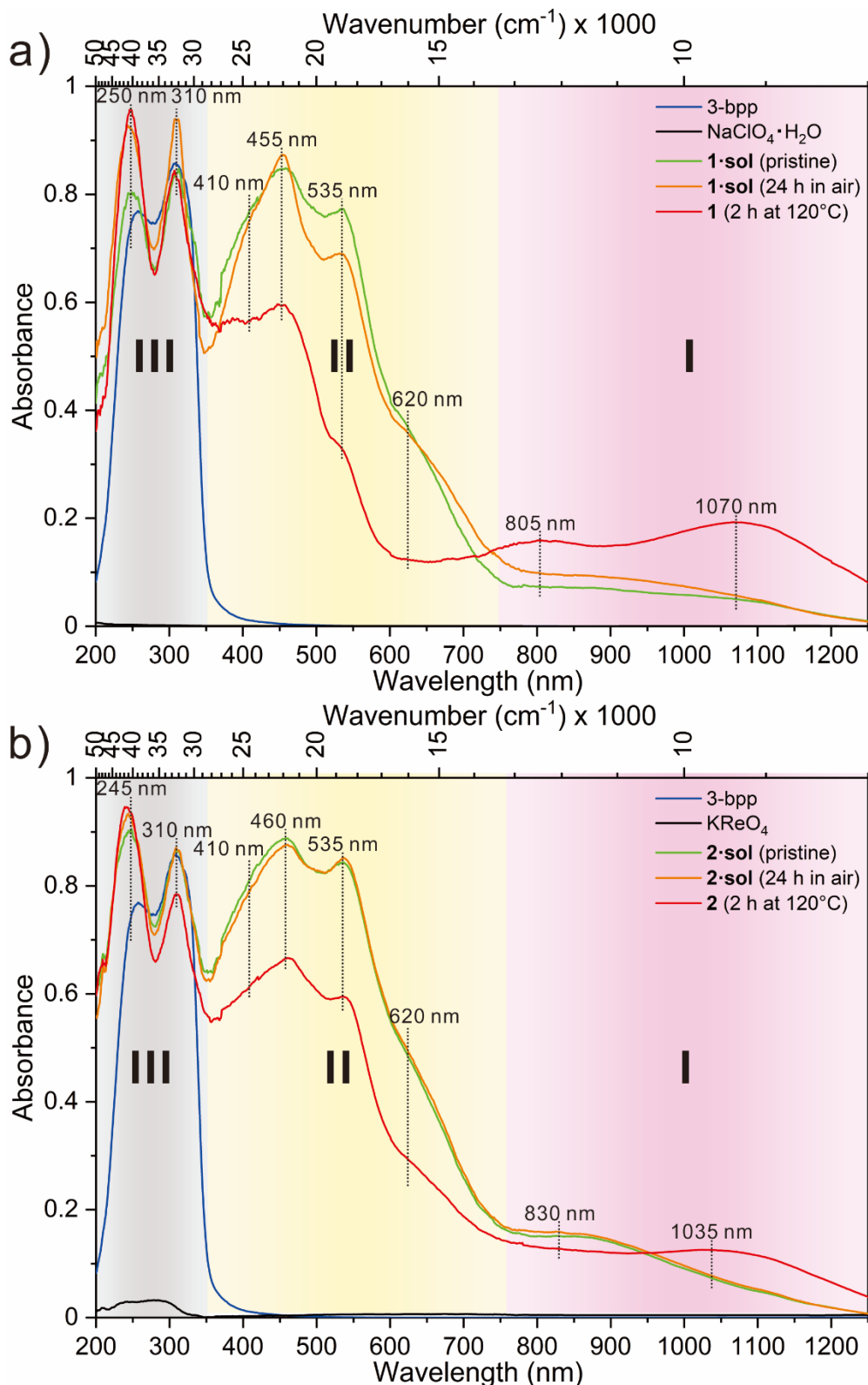


Figure S5. Room temperature solid–state UV–Vis–NIR absorption (Kubelka–Munk function) spectra with assignment of 3-bpp, $\text{NaClO}_4 \cdot \text{H}_2\text{O}$, KReO_4 , **1-sol** (a) and **2-sol** (b) (pristine, after 24 h in dry air, and 2 h heated at 120°C) dispersed in BaSO_4 .

Computational details

Quantum chemical calculations were done using Gaussian 16 software.^{R1} Input files were prepared based on the crystal structure of **1·sol** (90 K) and **2·sol** (250 K), and [Fe(3-bpp)₂][Au(CN)₂]₂·2H₂O (440 K)^{R2} by removing the solvents and anions forming model **A**, **B** and **C** (Figure S6). The single point DFT and TD-DFT calculations were performed with B3LYP functionals, using Karlsruhe type def2-SVP basis set for C, N and H atoms and triple-zeta def2-TZVP basis set for Fe(II) center.^{R3,R4} The calculation yielded model **A** and **B** with low spin (LS) configuration with similar UV-Vis-NIR spectra (Figure S7) and molecular orbitals (Figure S8), and model **C** with complete high spin (HS) configuration (Figure S9). Ground state to lowest 100 electronic excited states were calculated with oscillator strength magnetic moment and constituting molecular orbitals. The molecular arrangements for relevant excited levels are presented below for all three models.

References

- R1.** Gaussian 16, Revision B.01, M. J. Frisch, G. W. Trucks, H. B. Schlegel, G. E. Scuseria, M. A. Robb, J. R. Cheeseman, G. Scalmani, V. Barone, G. A. Petersson, H. Nakatsuji, X. Li, M. Caricato, A. V. Marenich, J. Bloino, B. G. Janesko, R. Gomperts, B. Mennucci, H. P. Hratchian, J. V. Ortiz, A. F. Izmaylov, J. L. Sonnenberg, D. Williams-Young, F. Ding, F. Lipparini, F. Egidi, J. Goings, B. Peng, A. Petrone, T. Henderson, D. Ranasinghe, V. G. Zakrzewski, J. Gao, N. Rega, G. Zheng, W. Liang, M. Hada, M. Ehara, K. Toyota, R. Fukuda, J. Hasegawa, M. Ishida, T. Nakajima, Y. Honda, O. Kitao, H. Nakai, T. Vreven, K. Throssell, J. A. Montgomery, Jr., J. E. Peralta, F. Ogliaro, M. J. Bearpark, J. J. Heyd, E. N. Brothers, K. N. Kudin, V. N. Staroverov, T. A. Keith, R. Kobayashi, J. Normand, K. Raghavachari, A. P. Rendell, J. C. Burant, S. S. Iyengar, J. Tomasi, M. Cossi, J. M. Millam, M. Klene, C. Adamo, R. Cammi, J. W. Ochterski, R. L. Martin, K. Morokuma, O. Farkas, J. B. Foresman, and D. J. Fox, Gaussian, Inc., Wallingford CT, 2016.
- R2.** A. Djemel, O. Stefanczyk, M. Marchivie, E. Trzop, E. Collet, C. Desplanches, R. Delimi and G. Chastanet, Solvatomorphism-Induced 45 K Hysteresis Width in a Spin-Crossover Mononuclear Compound, *Chem. Eur. J.*, 2018, **24**, 14760-14767.
- R3.** F. Weigend and R. Ahlrichs, Balanced basis sets of split valence, triple zeta valence and quadruple zeta valence quality for H to Rn: Design and assessment of accuracy, *Phys. Chem. Chem. Phys.*, 2005, **7**, 3297-3305.
- R4.** A. Schaefer, C. Huber and R. Ahlrichs, Fully optimized contracted Gaussian basis sets of triple zeta valence quality for atoms Li to Kr, *J. Chem. Phys.*, 1994, **100**, 5829.

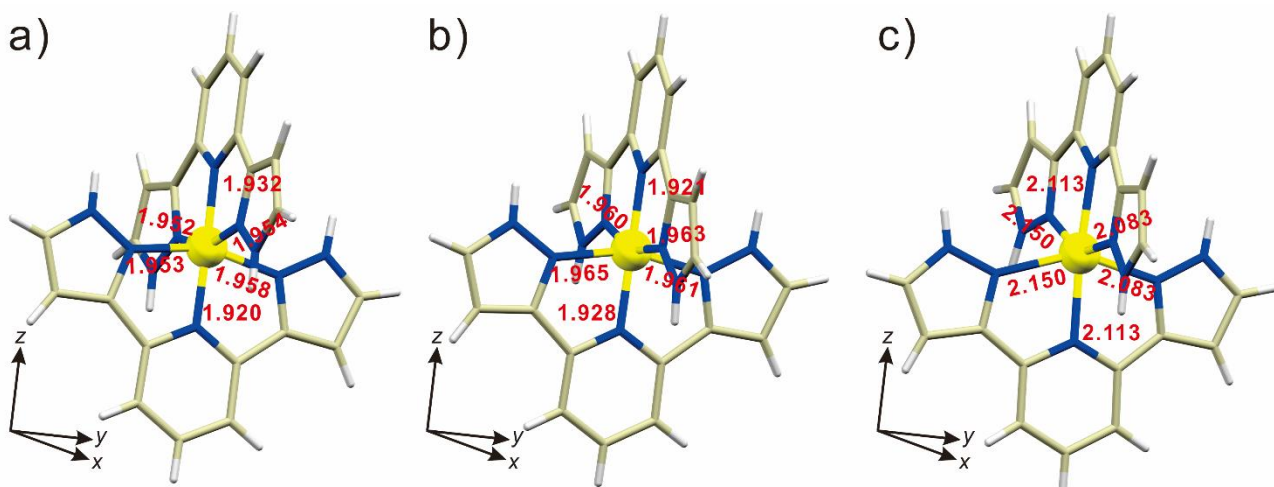


Figure S6. Models of **A** (a), **B** (b) and **C** (c) used for quantum chemical calculations. Legend: C – grey, Fe – yellow, H – white, and N – blue. Red numbers indicate bond lengths in the first coordination sphere of Fe(II) center.

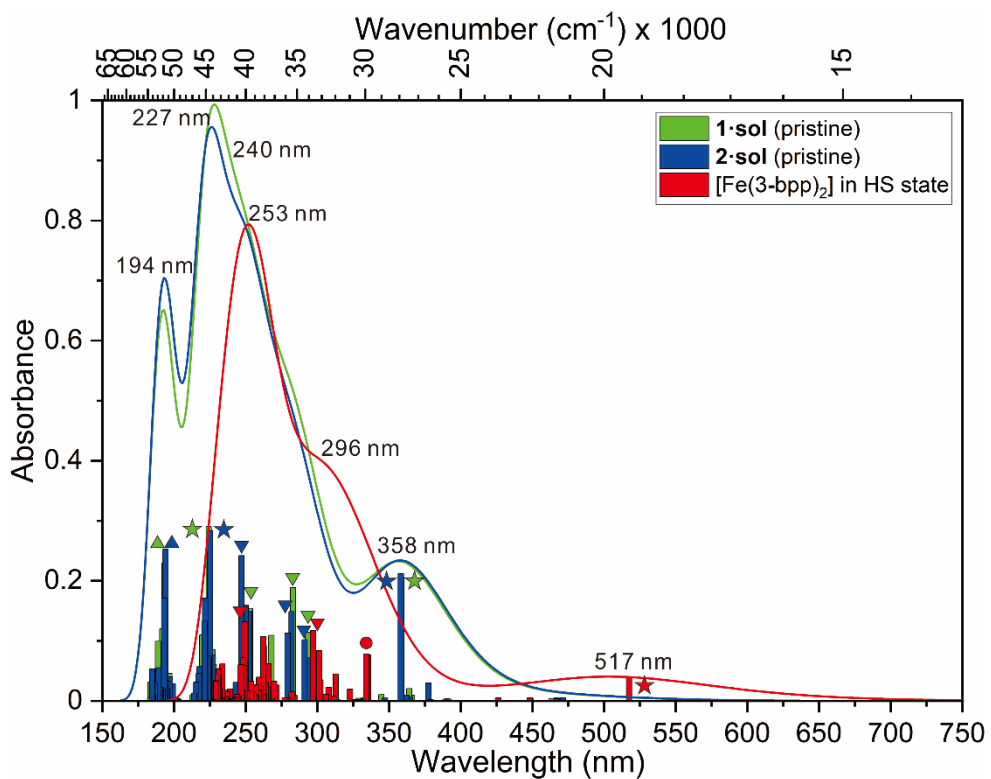


Figure S7. Calculated UV-vis spectra of **1-sol** (green), **2-sol** (blue), and $[\text{Fe}(3\text{-bpp})_2][\text{Au}(\text{CN})_2]_2 \cdot 2\text{H}_2\text{O}$ (red) base on models **A**, **B** and **C**, respectively. Bars indicate relative probability of electronic transitions. Symbols indicate electronic transitions with the largest contributions of: the *d-d* transitions and metal-to-ligand charge transfer (MLCT) - stars, ligand-to-ligand charge transfer (LLCT) – circles, MLCT and LLCT – down triangle, and ligand-to-metal charge transfer (LMCT).

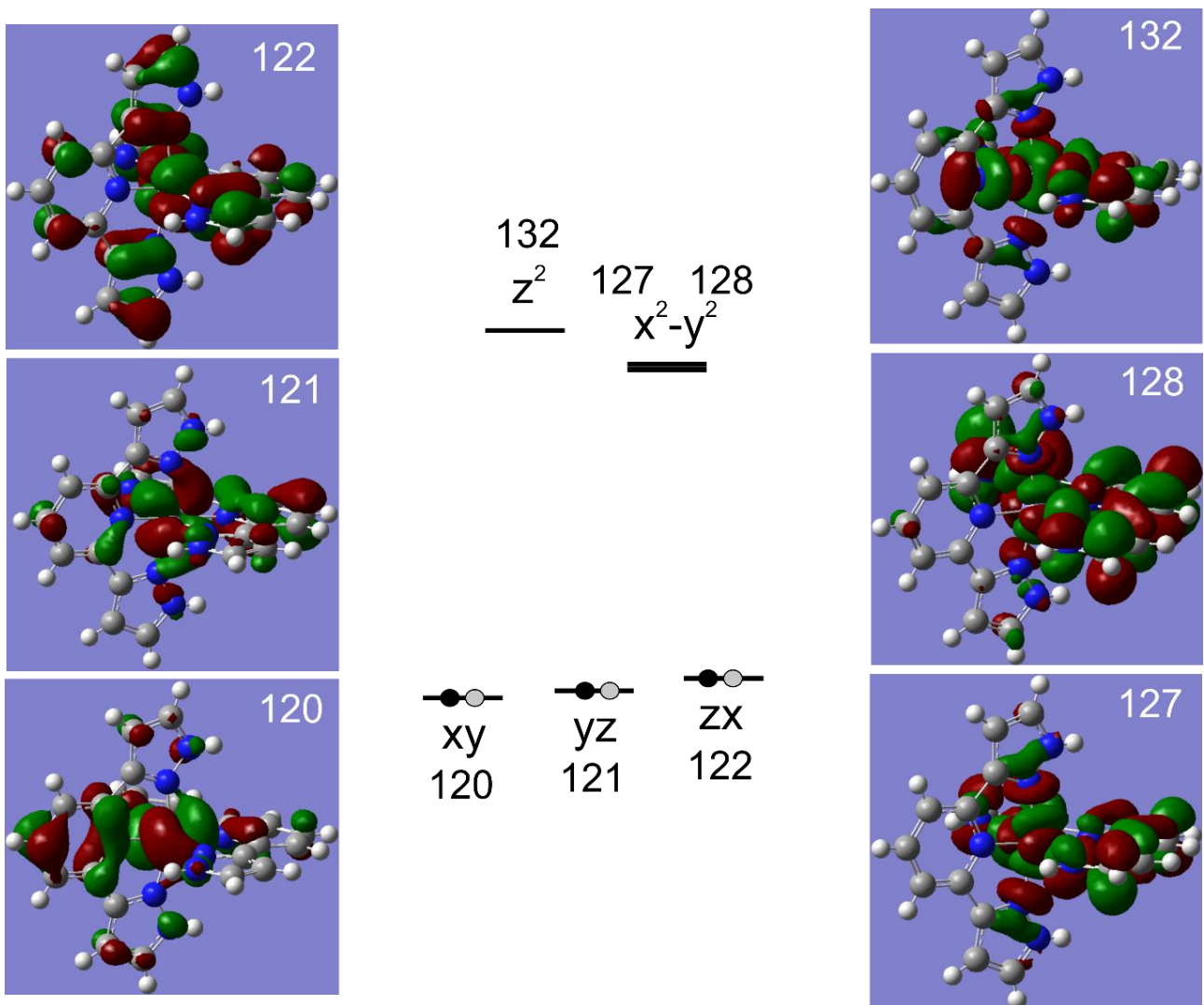


Figure S8. The energy level diagram with Fe *d*-based representative low spin molecular orbitals calculated for **1·sol** and **2·sol**.

List of excited state calculated for LS Fe(II)-based model **A** taken from complex **1·sol**.

Excited State 1:	Singlet-A	2.2226 eV	557.84 nm	f=0.0001	$\langle S^{**2} \rangle = 0.000$
112 ->127	0.15102				
118 ->127	-0.10202				
122 ->127	0.62113				
122 ->129	0.19782				
122 ->131	-0.10801				
Excited State 2:	Singlet-A	2.6554 eV	466.92 nm	f=0.0037	$\langle S^{**2} \rangle = 0.000$
120 ->127	0.27607				
120 ->130	0.22216				
122 ->123	0.58685				
Excited State 3:	Singlet-A	2.6760 eV	463.32 nm	f=0.0029	$\langle S^{**2} \rangle = 0.000$
121 ->127	0.33888				
121 ->129	0.14079				
121 ->130	-0.28310				
121 ->131	-0.10129				
121 ->132	0.15090				
122 ->124	0.46153				

Excited State 4: Singlet-A 2.7541 eV 450.18 nm f=0.0003 <S**2>=0.000
 120 ->127 0.28815
 120 ->130 0.49727
 120 ->132 -0.13549
 122 ->123 -0.35553
 Excited State 5: Singlet-A 2.7609 eV 449.06 nm f=0.0012 <S**2>=0.000
 121 ->127 -0.19145
 121 ->129 -0.10221
 121 ->130 0.37577
 121 ->132 -0.16184
 122 ->124 0.50436
 Excited State 6: Singlet-A 3.0546 eV 405.90 nm f=0.0005 <S**2>=0.000
 120 ->123 0.46656
 121 ->124 -0.32914
 122 ->130 0.35447
 122 ->132 -0.12394
 Excited State 7: Singlet-A 3.1519 eV 393.36 nm f=0.0000 <S**2>=0.000
 120 ->123 0.43792
 121 ->124 0.53886
 Excited State 8: Singlet-A 3.1753 eV 390.46 nm f=0.0027 <S**2>=0.000
 120 ->124 0.27398
 121 ->123 -0.27254
 122 ->125 0.56797
 122 ->126 0.11477
 Excited State 9: Singlet-A 3.2854 eV 377.38 nm f=0.0068 <S**2>=0.000
 120 ->124 -0.32133
 121 ->123 -0.40088
 122 ->125 -0.11361
 122 ->126 0.44605
 Excited State 10: Singlet-A 3.3876 eV 366.00 nm f=0.0069 <S**2>=0.000
 120 ->125 0.29654
 120 ->127 0.31088
 120 ->129 0.12531
 120 ->130 -0.22947
 120 ->132 0.11678
 121 ->125 0.39210
 121 ->127 -0.15348
 Excited State 11: Singlet-A 3.4054 eV 364.08 nm f=0.0154 <S**2>=0.000
 120 ->125 0.36172
 120 ->126 0.12111
 120 ->127 -0.11710
 121 ->125 -0.24863
 121 ->126 -0.10102
 121 ->127 -0.30987
 121 ->130 -0.28453
 122 ->126 0.19955
 Excited State 12: Singlet-A 3.4583 eV 358.51 nm f=0.1549 <S**2>=0.000
 120 ->124 0.35233
 121 ->123 0.31032
 121 ->125 0.15046
 122 ->126 0.43615
 Excited State 13: Singlet-A 3.5975 eV 344.64 nm f=0.0080 <S**2>=0.000
 120 ->123 -0.26632
 121 ->124 0.27201
 122 ->126 -0.13073
 122 ->130 0.51952

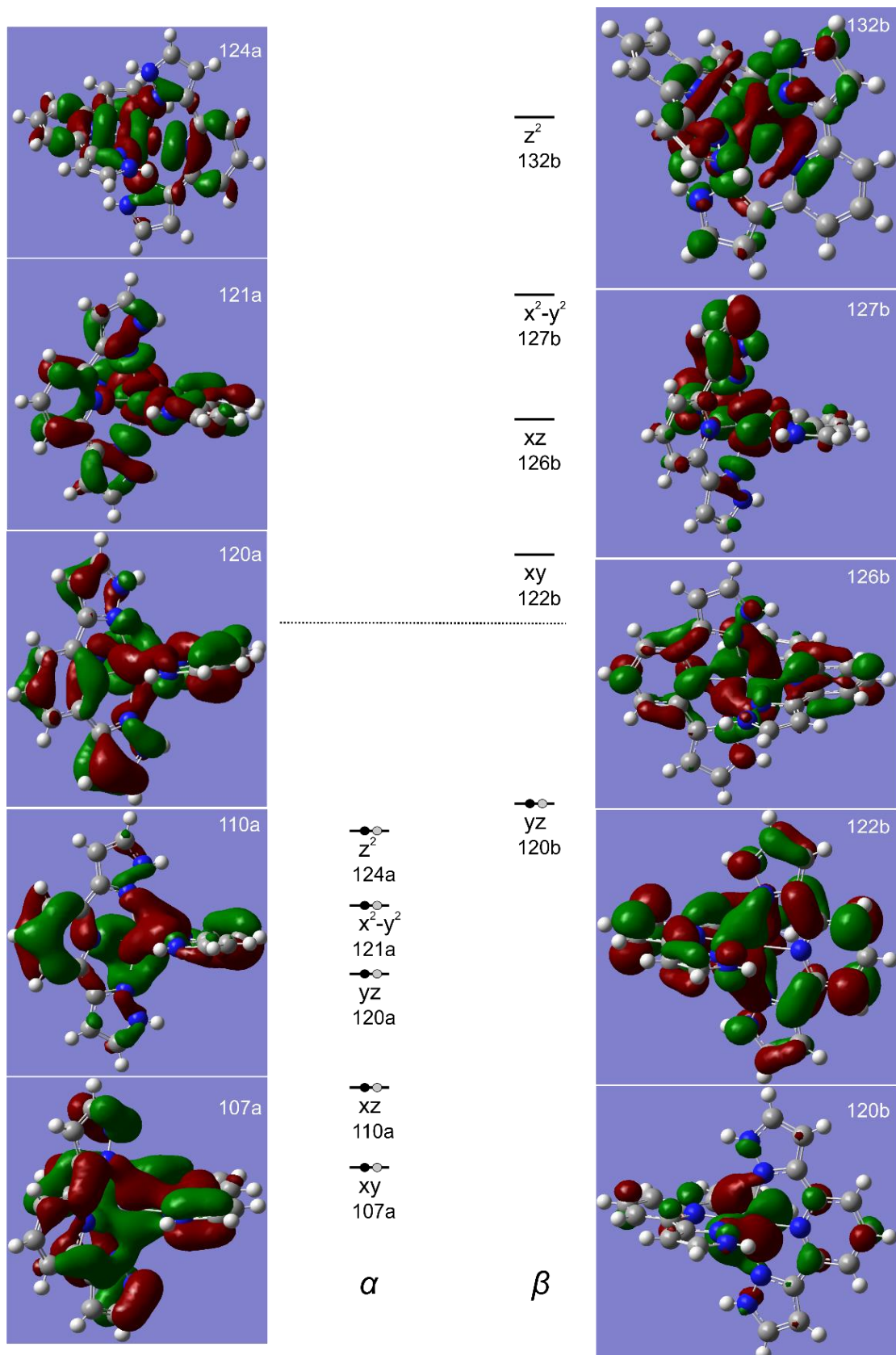
122 ->132 -0.18656
 Excited State 14: Singlet-A 3.7116 eV 334.04 nm f=0.0020 <S**2>=0.000
 120 ->125 0.37352
 120 ->126 -0.19304
 120 ->127 0.13922
 121 ->125 -0.32867
 121 ->126 0.16365
 121 ->127 0.28196
 121 ->130 0.20607
 Excited State 15: Singlet-A 3.7572 eV 329.99 nm f=0.0016 <S**2>=0.000
 120 ->125 0.29848
 120 ->127 -0.33362
 120 ->129 -0.12790
 120 ->130 0.21560
 120 ->132 -0.12495
 121 ->125 0.34634
 121 ->127 0.13787
 121 ->130 0.12888
 Excited State 16: Singlet-A 3.7720 eV 328.70 nm f=0.0034 <S**2>=0.000
 118 ->123 0.11036
 119 ->123 0.11470
 120 ->125 -0.10251
 120 ->126 0.19889
 121 ->125 -0.10723
 121 ->126 0.62054
 Excited State 17: Singlet-A 3.8240 eV 324.23 nm f=0.0010 <S**2>=0.000
 120 ->126 0.62173
 121 ->126 -0.14373
 121 ->127 0.17501
 121 ->130 0.14680

List of excited state calculated for LS Fe(II)-based model **B** taken from complex **2·sol.**

Excited State 1: Singlet-A 2.1807 eV 568.56 nm f=0.0000 <S**2>=0.000
 112 ->127 0.14573
 122 ->127 0.57693
 122 ->128 0.32367
 122 ->129 -0.11194
 Excited State 2: Singlet-A 2.6298 eV 471.46 nm f=0.0040 <S**2>=0.000
 120 ->127 0.25406
 120 ->128 0.13572
 120 ->132 -0.13052
 121 ->132 -0.14446
 122 ->123 0.53761
 122 ->124 -0.26630
 Excited State 3: Singlet-A 2.6543 eV 467.11 nm f=0.0028 <S**2>=0.000
 120 ->132 -0.20712
 121 ->127 0.30918
 121 ->128 0.18520
 121 ->132 0.21318
 122 ->123 0.24754
 122 ->124 0.41446
 Excited State 4: Singlet-A 2.7362 eV 453.13 nm f=0.0006 <S**2>=0.000
 120 ->127 -0.15838
 120 ->130 -0.14678

120 ->132	0.46141
121 ->127	-0.19564
121 ->128	-0.10723
122 ->123	0.35264
122 ->124	0.19617
Excited State 5:	Singlet-A 2.7465 eV 451.43 nm f=0.0008 <S**2>=0.000
120 ->127	0.21372
120 ->128	0.11743
121 ->130	0.14358
121 ->132	-0.42926
122 ->124	0.44289
Excited State 6:	Singlet-A 3.0260 eV 409.72 nm f=0.0001 <S**2>=0.000
120 ->123	0.45014
121 ->123	0.17790
121 ->124	-0.33150
122 ->130	0.11955
122 ->132	-0.34692
Excited State 7:	Singlet-A 3.1169 eV 397.77 nm f=0.0000 <S**2>=0.000
120 ->123	0.30425
120 ->124	-0.35251
121 ->123	0.29359
121 ->124	0.42959
Excited State 8:	Singlet-A 3.1913 eV 388.51 nm f=0.0012 <S**2>=0.000
120 ->123	-0.23674
120 ->124	-0.16867
121 ->123	0.26729
121 ->124	-0.12698
122 ->125	0.56711
Excited State 9:	Singlet-A 3.2852 eV 377.41 nm f=0.0225 <S**2>=0.000
120 ->124	0.41406
121 ->123	0.37345
121 ->124	0.12040
122 ->126	0.39435
Excited State 10:	Singlet-A 3.4002 eV 364.63 nm f=0.0045 <S**2>=0.000
120 ->127	-0.34556
120 ->128	-0.19989
120 ->132	-0.12863
121 ->125	0.45554
121 ->130	0.14467
121 ->132	-0.23827
Excited State 11:	Singlet-A 3.4234 eV 362.17 nm f=0.0076 <S**2>=0.000
120 ->125	0.43477
120 ->132	0.28703
121 ->127	0.34396
121 ->128	0.18084
121 ->132	-0.16296
122 ->126	-0.12676
Excited State 12:	Singlet-A 3.4606 eV 358.27 nm f=0.1590 <S**2>=0.000
120 ->123	0.11978
120 ->124	-0.23843
120 ->125	0.10090
121 ->123	-0.25863
121 ->124	-0.13309
122 ->126	0.55495
Excited State 13:	Singlet-A 3.5714 eV 347.16 nm f=0.0035 <S**2>=0.000
120 ->123	0.25045

120 ->124	0.11860			
121 ->124	-0.24810			
122 ->130	-0.18151			
122 ->132	0.53626			
Excited State 14:	Singlet-A	3.7304 eV	332.36 nm	f=0.0040 <S**2>=0.000
118 ->123	-0.10426			
120 ->125	0.36391			
120 ->127	-0.18305			
120 ->128	-0.11334			
120 ->132	-0.21194			
121 ->125	-0.33265			
121 ->126	-0.23969			
121 ->127	-0.20311			
121 ->128	-0.11523			
Excited State 15:	Singlet-A	3.7513 eV	330.51 nm	f=0.0016 <S**2>=0.000
120 ->125	0.34634			
120 ->127	0.22748			
120 ->128	0.12424			
121 ->125	0.37904			
121 ->127	-0.19390			
121 ->132	0.27152			
Excited State 16:	Singlet-A	3.7956 eV	326.65 nm	f=0.0015 <S**2>=0.000
120 ->125	0.10041			
120 ->126	-0.27997			
121 ->125	-0.13048			
121 ->126	0.58783			
Excited State 17:	Singlet-A	3.8110 eV	325.33 nm	f=0.0015 <S**2>=0.000
120 ->125	0.13588			
120 ->126	0.61862			
121 ->126	0.24556			



List of excited state calculated for HS Fe(II)-based model **C** taken from reference **R2**.

Excited State 1: 5.017-A 0.1740 eV 7124.97 nm f=0.0004 <S**2>=6.042
 120B ->121B 0.74774
 120B ->126B 0.67968
 120B <-121B 0.15524
 120B <-126B 0.15702

Excited State 2: 5.011-A 0.2950 eV 4203.22 nm f=0.0002 <S**2>=6.028
 120B ->122B 0.75908
 120B ->123B 0.13318
 120B ->125B 0.57158
 120B ->131B 0.16578
 120B ->132B 0.18888

Excited State 3: 5.000-A 1.7155 eV 722.72 nm f=0.0001 <S**2>=6.000
 120B ->127B 0.84813
 120B ->128B 0.47661
 120B ->130B -0.15646

Excited State 4: 5.003-A 2.1313 eV 581.72 nm f=0.0000 <S**2>=6.007
 120B ->125B -0.16668
 120B ->131B -0.41475
 120B ->132B 0.81282
 120B ->133B -0.16079
 120B ->135B -0.29016

Excited State 5: 5.455-A 2.3575 eV 525.91 nm f=0.0003 <S**2>=7.188
 120A ->126A -0.10392
 120B ->122B -0.18688
 120B ->123B 0.95429

Excited State 6: 5.408-A 2.3961 eV 517.45 nm f=0.0299 <S**2>=7.062
 120B ->121B -0.66704
 120B ->124B -0.14861
 120B ->126B 0.70549

Excited State 7: 5.118-A 2.6596 eV 466.17 nm f=0.0002 <S**2>=6.300
 124A ->125A 0.97989

Excited State 8: 5.110-A 2.6829 eV 462.12 nm f=0.0000 <S**2>=6.279
 124A ->126A 0.96370
 124A ->127A 0.16774

Excited State 9: 5.396-A 2.7612 eV 449.02 nm f=0.0034 <S**2>=7.029
 120B ->122B -0.61494
 120B ->123B -0.12213
 120B ->125B 0.73614
 120B ->132B 0.16750

Excited State 10: 5.397-A 2.7671 eV 448.06 nm f=0.0040 <S**2>=7.032
 120B ->124B 0.97645
 120B ->126B 0.15656

Excited State 11: 5.688-A 2.9102 eV 426.03 nm f=0.0039 <S**2>=7.839
 115A ->126A -0.13831
 116A ->125A -0.12369
 121A ->126A 0.15024
 121A ->127A -0.14218
 122A ->125A -0.27309
 122A ->128A 0.31079
 123A ->126A -0.27384
 123A ->127A 0.28160
 113B ->121B -0.10377
 115B ->123B -0.11020
 116B ->121B 0.13218

118B ->121B	0.31784
118B ->124B	0.30272
119B ->122B	0.46728
119B ->123B	-0.17908
119B ->125B	-0.12489
120B ->121B	0.10169
120B ->126B	-0.10172
Excited State 12:	5.683-A 2.9114 eV 425.86 nm f=0.0001 <S**2>=7.824
115A ->125A	0.13255
116A ->126A	0.12411
121A ->125A	-0.15074
121A ->128A	0.13270
122A ->126A	0.32575
122A ->127A	-0.28900
123A ->125A	0.24491
123A ->128A	-0.27338
124A ->127A	0.14401
115B ->121B	0.13863
116B ->123B	-0.10254
118B ->122B	0.39542
118B ->123B	-0.18495
118B ->125B	-0.11517
119B ->121B	0.39630
119B ->124B	0.31628
120B ->123B	-0.12038
Excited State 13:	5.340-A 3.1102 eV 398.63 nm f=0.0006 <S**2>=6.880
122A ->126A	-0.17189
122A ->127A	-0.14755
123A ->125A	-0.17677
123A ->128A	-0.16238
124A ->126A	-0.16288
124A ->127A	0.72705
118B ->122B	0.14282
118B ->123B	0.17216
119B ->121B	-0.45132
119B ->124B	0.13013
Excited State 14:	5.605-A 3.1658 eV 391.63 nm f=0.0024 <S**2>=7.604
121A ->126A	0.11651
122A ->125A	-0.31560
122A ->128A	-0.21093
123A ->126A	-0.24440
123A ->127A	-0.25443
124A ->128A	0.23204
118B ->121B	0.58741
118B ->124B	-0.17179
119B ->122B	-0.26724
119B ->123B	-0.30591
Excited State 15:	5.394-A 3.1719 eV 390.89 nm f=0.0009 <S**2>=7.024
121A ->128A	-0.16411
122A ->126A	0.12141
122A ->127A	0.27260
123A ->125A	0.13849
123A ->128A	0.16938
124A ->127A	0.63281
118B ->122B	-0.25108
118B ->123B	-0.15477

119B ->121B	0.44897
119B ->124B	-0.21005
Excited State 16:	5.134-A 3.2718 eV 378.95 nm f=0.0017 <S**2>=6.339
121A ->127A	-0.15791
122A ->128A	0.10457
124A ->128A	0.94909
118B ->121B	-0.12656
119B ->122B	0.11411
Excited State 17:	5.097-A 3.5884 eV 345.52 nm f=0.0005 <S**2>=6.244
121A ->125A	0.75353
122A ->126A	0.11324
123A ->125A	0.60398
124A ->126A	0.11127
119B ->121B	-0.14660
Excited State 18:	5.083-A 3.6138 eV 343.09 nm f=0.0002 <S**2>=6.210
121A ->126A	0.87331
121A ->127A	0.11538
122A ->125A	-0.12058
123A ->126A	0.41435
124A ->125A	0.11309
Excited State 19:	5.228-A 3.6967 eV 335.39 nm f=0.0574 <S**2>=6.583
121A ->125A	0.43302
122A ->126A	-0.41232
122A ->127A	-0.14213
123A ->125A	-0.27842
118B ->123B	0.26182
119B ->121B	0.62326
119B ->126B	0.13319
Excited State 20:	5.255-A 3.7120 eV 334.01 nm f=0.0587 <S**2>=6.654
118A ->125A	0.10228
122A ->125A	0.38586
123A ->126A	0.37951
115B ->122B	-0.10462
116B ->124B	-0.11912
118B ->121B	0.70500
118B ->126B	0.10910
119B ->123B	0.27478

Single crystal X-ray diffraction (SCXRD) studies

Table S1. Selected crystallographic parameters for **1·sol** and **2·sol**.

	1·sol	2·sol
Formula	C _{22.5} H ₂₀ Cl ₂ FeN ₁₀ O ₁₁	C ₂₂ H ₂₄ FeN ₁₀ O ₁₁ Re ₂
M _w (g/mol)	733.23	1032.76
T (K)	90(2)	250(2)
Crystal system, space group	Triclinic, <i>P</i> -1	Triclinic, <i>P</i> -1
<i>a</i> (Å)	8.2930(5)	11.6404(4)
<i>b</i> (Å)	8.3598(6)	11.8143(4)
<i>c</i> (Å)	21.9377(13)	11.9919(4)
α (°)	81.870(6)	107.9610(10)
β (°)	89.641(6)	99.9260(10)
γ (°)	89.552(6)	91.0420(10)
<i>V</i> (Å ³)	1505.54(17)	1540.83(9)
<i>Z</i>	2	2
ρ_{calc} (g/cm ³)	1.617	2.226
μ (mm ⁻¹)	0.753	8.374
<i>F</i> (000)	746	980
Crystal size (mm ³)	0.262 × 0.174 × 0.100	0.314 × 0.120 × 0.111
Radiation	MoK _α (λ = 0.71075)	MoK _α (λ = 0.71075)
2θ range (°)	6.198 to 54.97	4.25 to 55.064
Index ranges	-10 ≤ <i>h</i> ≤ 9, -10 ≤ <i>k</i> ≤ 10, -28 ≤ <i>l</i> ≤ 28	-15 ≤ <i>h</i> ≤ 15, -15 ≤ <i>k</i> ≤ 14, -15 ≤ <i>l</i> ≤ 15
Reflections collected / unique	14694 / 6865 [$R_{\text{int}} = 0.0588$, $R_{\text{sigma}} = 0.0812$]	38720 / 7089 [$R_{\text{int}} = 0.0318$, $R_{\text{sigma}} = 0.0264$]
Refinement method	Full-matrix least-squares on F^2	Full-matrix least-squares on F^2
Data/restraints/parameters	6865/148/500	7089/0/424
GOF on F^2	1.205	1.097
R_1/wR_2 ($ I > 2\sigma(I)$)	0.1084/0.2077	0.0357/0.0912
R_1/wR_2 (all data)	0.1339/0.2198	0.0504/0.0992
Largest diff. peak and hole (e/Å ³)	1.28/-0.94	2.15/-2.61
CCDC number		

Table S2. Selected bond lengths and angles for **1·sol** and **2·sol**.

	1·sol	2·sol
Bond lengths (Å)		
Fe1-N1 _{pyr}	1.951(5)	1.959(5)
Fe1-N2 _{py}	1.930(5)	1.920(5)
Fe1-N3 _{pyr}	1.955(5)	1.963(5)
Fe1-N4 _{pyr}	1.957(4)	1.961(5)
Fe1-N5 _{py}	1.921(5)	1.928(5)
Fe1-N6 _{pyr}	1.952(4)	1.965(5)
Fe-N_{aver}	1.944(5)	1.949(5)
Angles (°)		
N1 _{pyr} -Fe1-N2 _{py}	78.9(2)	79.4(2)
N2 _{py} -Fe1-N3 _{pyr}	79.4(2)	79.7(2)
N4 _{pyr} -Fe1-N5 _{py}	79.3(2)	79.3(2)
N5 _{py} -Fe1-N6 _{pyr}	79.2(2)	79.4(2)
(N _{pyr} -Fe-N _{py}) _{aver}	79.2(2)	79.5(2)
N1 _{pyr} -Fe1-N4 _{pyr}	91.79(19)	91.6(2)
N1 _{pyr} -Fe1-N6 _{pyr}	91.96(19)	91.3(2)
N3 _{pyr} -Fe1-N4 _{pyr}	92.55(19)	92.0(2)
N3 _{pyr} -Fe1-N6 _{pyr}	91.73(19)	92.8(2)
(N _{pyr} -Fe-N _{pyr}) _{aver}	92.00(19)	91.9(2)

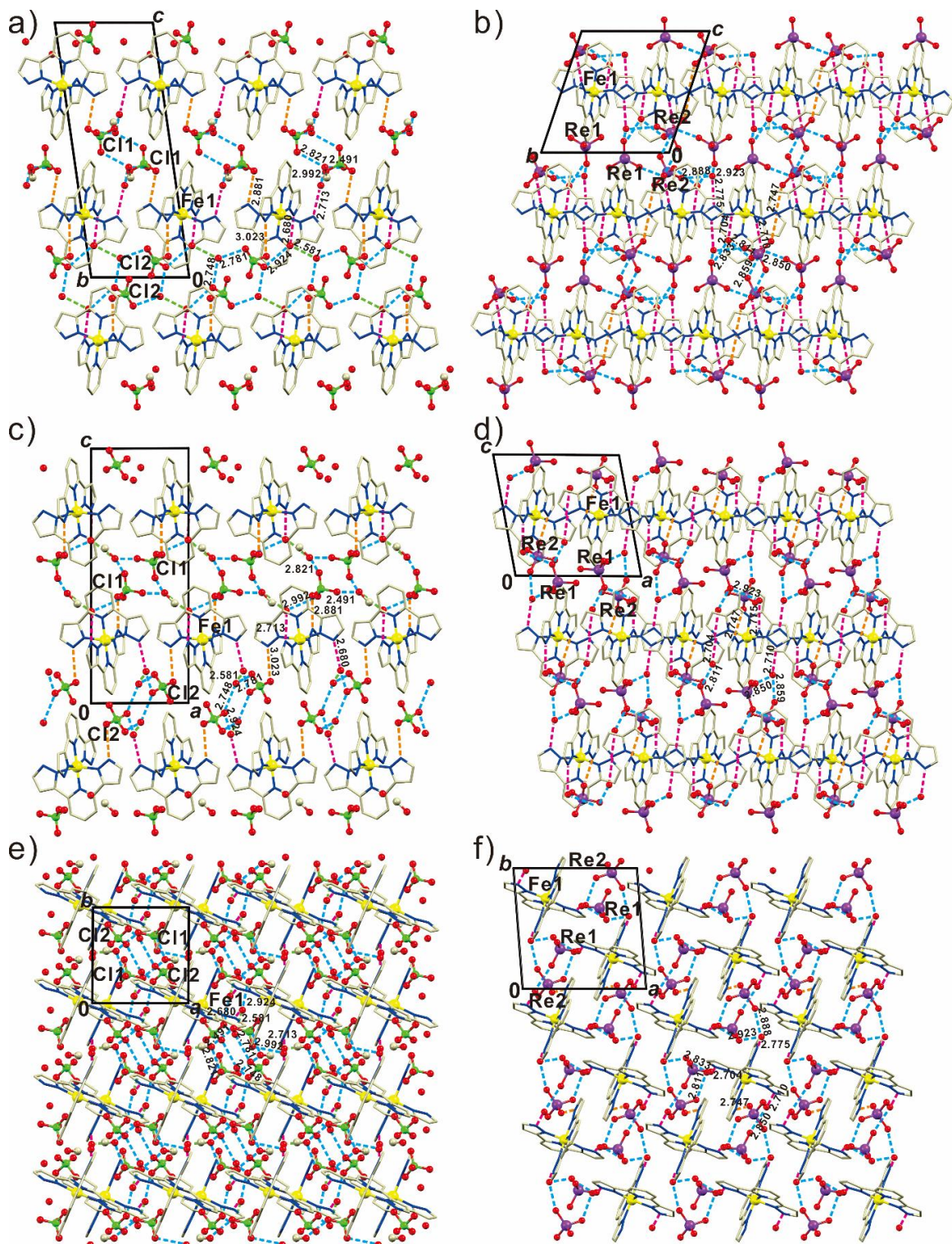


Figure S10. Packing along crystallographic directions (100) (**a** for **1-sol** and **b** for **2-sol**), (010) (**c** for **1-sol** and **d** for **2-sol**), and (001) (**e** for **1-sol** and **f** for **2-sol**) including a hydrogen bond networks between 3-bpp and XO_4^- anions (orange dashed lines), 3-bpp and water molecules (magenta dashed lines), water molecules and XO_4^- anions (blue dashed lines), and in solvent molecules (green dashed lines). The numbers correspond to the distances between the hydrogen bond donor and acceptor. For clarity, hydrogen atoms have been omitted.

Powder X-ray diffraction (PXRD) studies

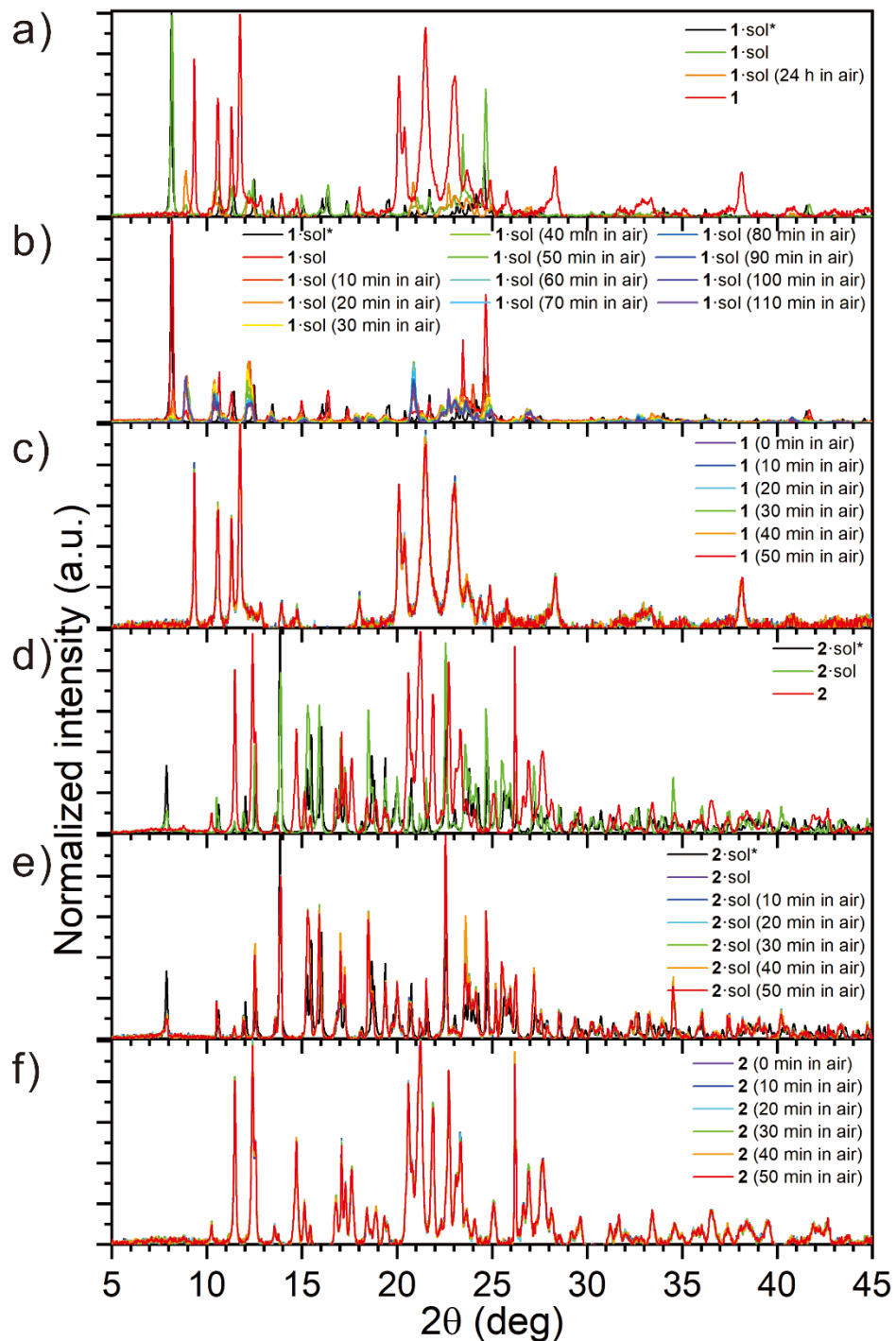


Figure S11. (a) Experimental PXRD patterns of **1-sol** (pristine, after 24 h in dry air, and 2 h heated at 120°C) and calculated from single-crystal X-ray diffraction data including texture effect with preferred platy orientation along (002) direction with March-Dollase parameter $M/D = 0.6$ (**1-sol***). (b) Time-evolution of diffractograms of pristine **1-sol**. (c) Time-evolution of PXRD patterns of desolvated **1** (2 h heated at 120°C). (d) Experimental PXRD patterns of **2-sol** (pristine and 2 h heated at 120°C) and calculated from single-crystal X-ray diffraction data (**2-sol***). (e) Time-evolution of diffractograms of pristine **2-sol**. (f) Time-evolution of PXRD patterns of desolvated **2** (2 h heated at 120°C).

Photomagnetic properties

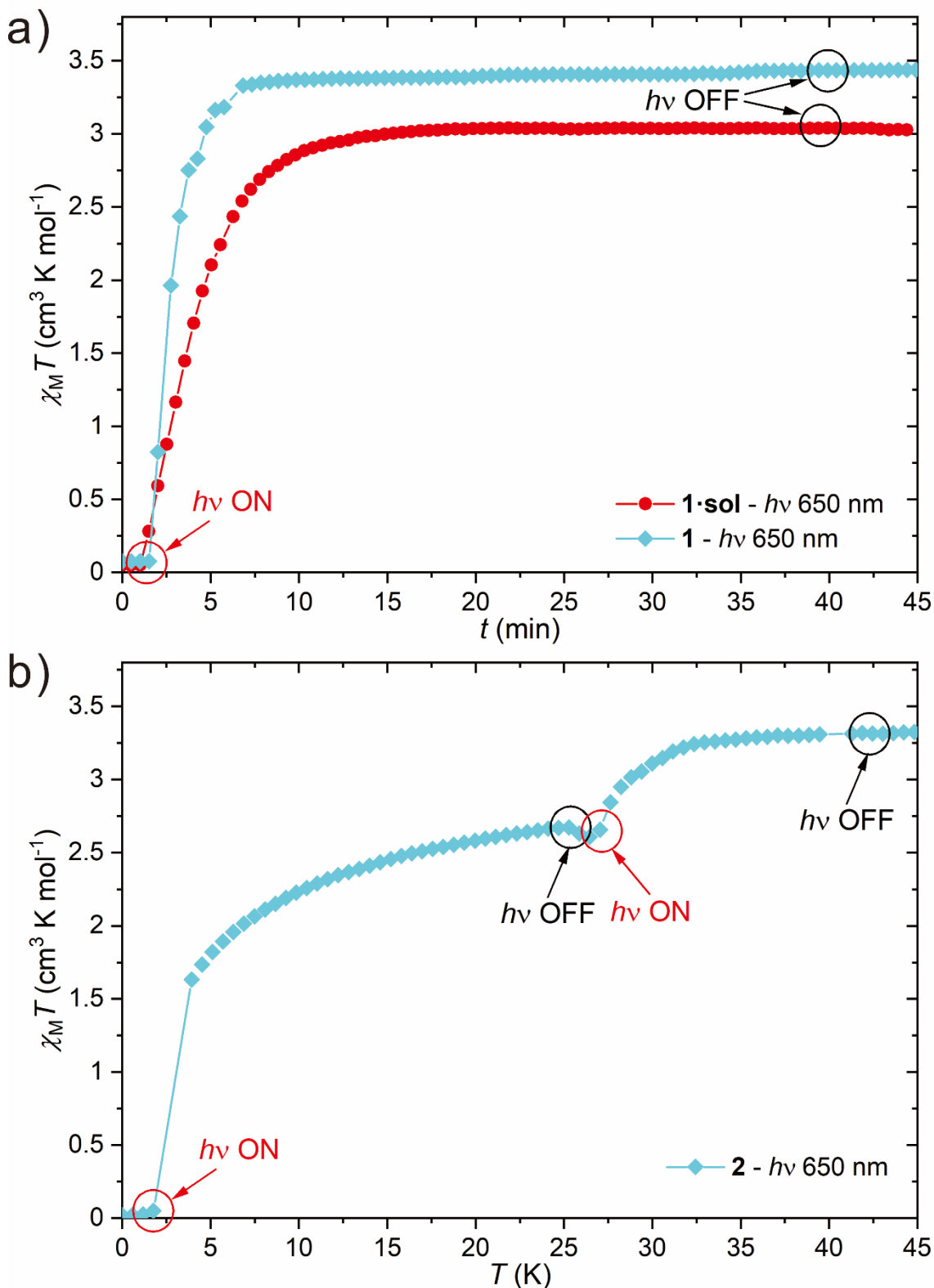


Figure S12. Time dependence of $\chi_M T$ at $H_{dc} = 10$ kOe during excitation at 10 K with 650 nm light ($P = 5$ mW/cm 2) for pristine ($1\cdot\text{sol}$) and desolvated phases (**1** and **2**).